



SolarPACES 2013

Comparison of 3 heat flux gauges and a water calorimeter for concentrated solar irradiance measurement

Emmanuel Guillot^{1,*}, Ivo Alxneit², Jesus Ballestrin³, Jean Louis Sans¹, Christian Willsh⁴

¹CNRS-PROMES, 7 rue du Four Solaire, 66120 Font Romeu Odeillo, France

²PSI, Solar Technology Laboratory, 65232 Villigen PSI, Switzerland

³CIEMAT-PSA, Plataforma Solar de Almería, Central Receiver Technology, P.O. Box 22, 4200 Tabernas, Almería, Spain

⁴DLR, Institut für Technische Thermodynamik, Solarforschung, Linder Höhe, 51147 Köln, Germany

Abstract

Heat flux gauges are widely used directly or to calibrate camera imaging system in order to determine the flux density and incident power of concentrated solar plants. Several laboratories have developed techniques to calibrate these sensors but with varying procedures and apparatus. No recent work has been conducted to check the degree of agreement between the calibrations from different laboratories for solar applications [1] [2].

This paper describes the results of the comparison of 4 sensors: 3 Gardon heat flux gauges and a water calorimeter were compared at the Big Solar Furnace in Odeillo for varying heat flux density and incoming angles up to 1500 kW/m² and 25 to 80°. Two Vatell commercial gauges had been calibrated with an electric heated radiative plate. One of them had been further corrected for the spectral distribution difference between the radiative plate (mostly infrared) and concentrated solar applications (mostly visible) [3]. One HyCal commercial gauge had been calibrated against a Kendall water-cooled absolute radiometer. The water calorimeter was representing cavity absolute radiometers exhibiting total apparent absorptivity.

We have observed an agreement within 10 % of all the sensors, but with a separation in two subgroups: on one hand the radiative plate calibrated gauges agreeing each around 1%, solar corrected or not, and on another hand the radiometer calibrated gauge and the water calorimeter. Additional experimental findings concerning angular response are also presented.

© 2013 The Authors. Published by Elsevier Ltd. This is an open access article under the CC BY-NC-ND license (<http://creativecommons.org/licenses/by-nc-nd/3.0/>).

Selection and peer review by the scientific conference committee of SolarPACES 2013 under responsibility of PSE AG.

Final manuscript published as received without editorial corrections.

Keywords: calibration; concentrated solar flux; Gardon gage; water calorimeter; solar furnace

* Corresponding author. Tel.: +33 4 68 30 77 56 ; fax: +33 4 68 30 77 99.

E-mail address: emmanuel.guillot@promes.cnrs.fr

1. Introduction

We present here our last comparison work to check the variations of measured concentrated solar power density as determined from several sensors calibrated in different conditions: there are currently no established norm for such solar plant power measurements at focus. Different measuring techniques and different calibration methods have been developed over the years, we have aimed here at comparing latest versions of some of them: Gardon sensors and water calorimeter, calibration on radiative plate with a solar corrected factor.

We also propose here a novel method for such comparison under concentrated solar energy in order to mitigate or discard the dependency of the atmospheric changes and the tracking errors by performing simultaneous measurements from the sensors and compare the calibration factors for a flux mapping camera system.

We have gathered 4 sensors for the test campaign, their identification and principal characteristics can be found in Table 1: one cavity water calorimeter, three flat Gardon sensors with three different calibration procedures.

Nomenclature

DNI	ground measurement of the solar Direct Normal Irradiation (W/m^2)
CSR	CircumSolar Ratio: ratio of solar energy inside the normalised sized solar disc surface and 2.5° around it
ΔT	Temperature difference between inlet cold water and outlet hot water of a calorimeter
Q	Water mass flow inside a calorimeter
Cp	Sensible heat of the water inside a calorimeter

Table 1. List of sensors used.

Sensor identification	Manufacturer	Serial Number	Type	Calibration
CNRS Idefix (France)	CNRS-PROMES	N/A	water calorimeter	ΔT with K thermocouples class I and Gantner A4, mass flow with Siemens Coriolis, 15.85 mm diaphragm
DLR (Germany)	Hycal	941347	16 mm Gardon	DLR 2940.78 $kW \cdot m^{-2} \cdot mV^{-1}$
CIEMAT (Spain)	Vatell	7481	25.4 mm Gardon	CIEMAT 120.48 $kW \cdot m^{-2} \cdot mV^{-1}$
PSI (Switzerland)	Vatell	9260	25.4 mm Gardon	Vatell 200.9 $kW \cdot m^{-2} \cdot mV^{-1}$
Voltage acquisition for all the Gardon sensors	Gantner	353428	A4	Manufacturer 2012
Temperature acquisition for CNRS Idefix calorimeter	Gantner	353427	A5 with cold junction compensation	Manufacturer 2012
Water mass flow for CNRS Idefix calorimeter	Siemens	7ME410 97401N075	Coriolis, Sitrans FC Massflo Mass 2100	France Métrologie Mars 2012
Pyrheliometer used for DNI	Kipp & Zonen	120880	CHP 1	Manufacturer 08-03-2012
Voltage acquisition for DNI	Gantner	N/D	A4	Manufacturer 2010

1.1. Flat Gardon radiometers

The transducer of these sensors consists of a differential thermocouple that measures the temperature difference between the center and the circumference of a thin foil disk, the diameter and thickness of which determines the range of irradiance that can be measured [5]. The disk is bonded to a circular opening in a 25.4 mm long cylindrical heat sink with a 7.9-25.4 mm front-face diameter. The standard foil is made of constantan and the heat sink is copper. These materials produce a voltage output which is directly proportional to the heat flux absorbed. The usual signal is 0-10 mV regardless of the heat flux range, which corresponds to a constantan-copper temperature difference of up to 214 °C. Gardon radiometers are fast sensors, with a typical response time slightly below 1 second.

One of the few suppliers of Gardon-type sensors is the Vatell Corporation. The exposed face of their sensors is sprayed with a highly absorbing black coating to achieve absorption high enough to generate a significant signal. Zynolyte® [3] is the preferred coating at Vatell because it creates a rough surface that improves absorption. However, for radiative fluxes higher than about $3500 \text{ kW}\cdot\text{m}^{-2}$ colloidal graphite (Electrodag® 154) is a better option because the center of the absorbing surface becomes hot enough for Zynolyte® to start to decompose.

1.1.1. Gardon radiometers: radiative plate calibration (PSI's sensor)

The current procedure for calibrating these sensors at Vatell is based on a dual-cavity black body, which is basically an electrically heated double-ended cylindrical graphite tube with a center partition that allows its internal temperature to be measured with a NIST-traceable pyrometer while the reference transducer is being calibrated. When the selected temperature of 850°C has stabilized, the transducer is quickly inserted into the cavity opposite the pyrometer. The Stefan-Boltzman law supplies the resulting irradiance value of about $90 \text{ kW}\cdot\text{m}^{-2}$ on the front face of the sensor, assuming hemispherical irradiation. Calibration of the reference heat flux sensor is performed with this single-point technique. This calibration is transferred to the commercial sensors by comparison in a calibration furnace with a graphite plate that radiates evenly and symmetrically when an electrical current passes through it. The calibration constant obtained with this method translates voltage to irradiance on the front face of the sensor. The manufacturer states that the accuracy of gages calibrated in this way is within $\pm 3\%$ with a repeatability of $\pm 1\%$ [3]. The PSI's sensor is a Gardon type radiometer manufactured and calibrated by Vatell, coated with Zynolyte®.

1.1.2. Gardon radiometers: solar corrected radiative plate calibration (CIEMAT's sensor)

These heat flux sensors are used in different fields such as plasma diagnostics and combustion research, which have to deal with dissimilar spectral radiances and, therefore, compatibility with solar radiation is not given, as the spectral absorptance of the coating is not constant over the relevant region of the electromagnetic spectrum. At 850°C , the spectral radiance of a black body is significantly different from the solar spectral distribution that corresponds roughly to a diluted black body spectrum of 6000°C . Thus, a systematic error arises due to the difference in power absorbed by the coatings under these two dissimilar electromagnetic spectral distributions [3, 4]. The systematic error from measuring solar irradiance with these gages has been estimated from all this information in previous articles [3, 4]: if the sensor coating is Zynolyte®, the sensor overestimates the solar irradiance by 3.6%.

The CIEMAT's sensor is a Gardon type radiometer manufactured and calibrated by Vatell, coated with Zynolyte®. The constant calibration supplied by Vatell was $124.85 \text{ kW}\cdot\text{m}^{-2}\cdot\text{mV}^{-1}$ but a corrected calibration constant of $120.48 \text{ kW}\cdot\text{m}^{-2}\cdot\text{mV}^{-1}$ is used by CIEMAT to measure solar radiative fluxes instead.

1.1.3. Gardon radiometers: Kendall calibration under concentrated solar flux (DLR's sensor)

Another possibility to mitigate the spectral effect of the source is directly to calibrate the sensor with solar energy. Colleagues at DLR's Köln solar furnace routinely calibrate Gardon radiometers using a Kendall total radiation absolute radiometer [6] as reference: both sensors are placed sequentially under concentrated irradiated solar flux thanks to a fast 3D moving platform. The required flux range is scanned by changing the position of the sensors in the focal volume and eventually by masking mirrors of the concentrating parabola or installing in the beam path intercepting devices such as meshes. This method has been used and described during the last comparison campaign in 2006 [2]. The accuracy of this method depends on the performance of the reference radiometer and on the characteristics of the atmosphere. DLR has declared this Kendall radiometer as its internal reference notably because it integrates an electric heating element that allows calibration of the thermal transfers of the instrument. However, the radiative to thermal transfer ratio is still determined by calculation of the apparent absorptivity of the black coated cavity.

1.2. Water calorimeter (CNRS's sensor)

Water calorimeters are absolute radiometers where all probed solar energy is absorbed in a black body cavity surrounded by a flowing heat transfer fluid, typically water for calorimeters used in solar furnaces. Measurement of the mass flow and of the thermal balance of this fluid allows to calculate the power transmitted to the fluid [7,8].

The performance of these devices is determined mainly by the accuracy of the flow and temperature measurements, but also on the design of the calorimeter cavity itself:

- The apparent absorptivity of the sensor depends strongly on the shape of the cavity and its coating which should be matched to the angular and spectral distribution of the incoming beam.
- The thermal balance depends on the ratio of thermal energy transmitted to the fluid compared to the energy lost notably by convection on the outside casing.
- Calculation of power density requires a very well defined aperture area (notably no denting, edge angle matching the incoming beam characteristics)
- The heat capacity of the fluid should be well known, including its temperature variation.

The CNRS's Idefix calorimeter has been designed for local measurements of the high power density of the Big Solar Furnace in Odeillo: up to 10000 kW.m⁻². It consists of a cavity formed by closely wound copper tubing (4 mm inner diameter) with external insulation in nylon. The cavity formed is 20 mm in diameter and 80 mm deep. The apparent cavity absorptivity was calculated to be higher than 99% for incident radiation from 20 to 80° as delivered by this furnace. A nickel coated polished copper foil diaphragm forms a well defined round aperture (15.85 mm diameter). This diaphragm is freely water-cooled on its outside edges.

The response time of a calorimeter varies depending on the flow rate of the heat transfer fluid. Typical response times for a full range step spans from a few seconds to 2 minutes. The Idefix calorimeter was operated in this study with a low water flow, requiring about 30 s before the readings stabilize.

2. Solar comparison methods of flux measurement sensors

In order to compare the measurements of the sensors, two methods have been discussed by the team: either a sequential or a simultaneous method.

2.1. Sequential method

The sequential method is the typical method applied in most comparisons: The sensors are installed one after the other at the same position within the focal region of the solar furnace. Only one sensor is therefore used at a particular time and one must wait sufficiently long depending on the rise time of the signals before starting to collect data. Measurement of a complete group of sensors for one point can therefore take 5-10 minutes even with a motorized setup if it includes slow sensors such as calorimeters. Repeated measurements at different flux levels or configuration as here can easily require several days of measurement time.

Nevertheless, this setup is the easiest to realize as it only requires an accurate system to change the position of the sensors. However, as each sensor is used sequentially, the method is sensitive to changes of the irradiance due e.g. to changing atmospheric conditions or to tracking errors. Pyrheliometer measurements are used to compensate for a variation of the DNI, but other perturbations such as e.g. changes of the circumsolar ratio (CSR) are usually not compensated. Compensation for a variable CSR requires complex instrumentation [9] such as e.g. the SAM (Solar Aureole Measurement system) manufactured by Visidyne currently being commissioned in Odeillo. The calibration errors of all these instruments used to correct the response of the sensor will influence the final results. Only if their calibration is excellent and stable can the correction be performed.

Atmospheric conditions at Odeillo can change within minutes, notably due to high altitude winds, undetectable from ground. A change in CSR can reduce the concentration ratio for high concentration solar plants up to about 10% despite stable pyrheliometer readings [10]. Small changes in the terrestrial solar spectrum will impede sensors with a narrow spectral response such as photonic sensors or with non flat spectral response. Note, that even black paints exhibit a non-flat absorption if the whole solar spectral range from the UV to the NIR is considered.

2.2. Simultaneous method

The simultaneous method as proposed by CIEMAT aims at solving the issues of the sequential method. All the sensors are installed simultaneously at the focal plane and measurements are made continuously. A Lambertian reflective moving target such as described in [11] is placed periodically in front of the sensors and a camera is used to measure the gray level associated to an irradiance value at the position of each sensor. Comparing the curves (gray level vs irradiance) of all sensors would allow us to compare these devices in an objective way without the need for a reference sensor. Care has to be taken to ensure that the camera displays no spatial inhomogeneity.

This setup requires the use of a camera, a Lambertian target that can be moved in front of the sensors, a big focal area allowing to expose all the sensor in similar flux conditions. The camera's performance must be characterized beforehand in terms of relative spatial sensitivity and temporal stability. The spatial sensitivity is notably affected by the optical system used and the properties of the Lambertian target while the temporal stability is mostly affected by the temperature stability of the CCD sensor used in the camera. Uncertainties due to the spatial inhomogeneity can be reduced by exchanging sensors position, hence increasing the time required for the tests.

Different radiometers and calorimeters to be compared

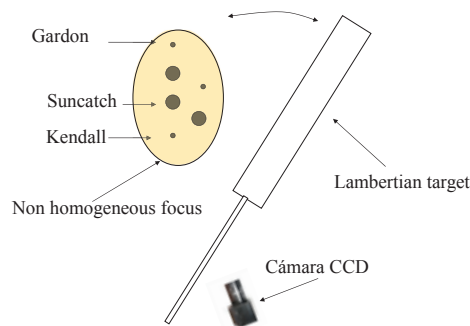


Fig. 1. Principle of the simultaneous method: all the sensors continuously and simultaneously measure the concentrated incoming flux. A camera imaging system with a Lambertian moving target is used to correct for the non-homogeneities in the flux distribution of the focal place.

2.3. Method selected

In order to also study the dependence of the angular distribution of the incoming radiation on the sensors, the CNRS Big Solar Furnace in Odeillo, France, has been selected as it allows both to cover the desired power range ($0-1500 \text{ kW}\cdot\text{m}^{-2}$) and the desired range of angles of the incoming radiation (as large as possible — available at Odeillo: 25 to 80° from normal), by selecting suitable configurations of the solar furnace (see Appendix A).

As the Big Solar Furnace's new camera based flux measurement system "PETALES" is not yet qualified to guarantee sufficient repeatability and low enough uncertainty, the sequential method has been selected as for the previous campaign by the team in 2006 at the DLR Köln Solar Furnace [2].

The stability of the spectral atmospheric absorption is assumed acceptable by choosing clear sky days for the measurements as done in previous campaign. The terrestrial solar radiation was not characterized spectrally nor was the CSR determined. As all the sensors are reference sensors with wide spectrum black paint as absorbers, the effect of spectral variation are considered negligible. The extent of the validity of these assumptions has not been verified; we have only repeated our typical best practices: low diffuse horizontal radiation ($<60 \text{ W}/\text{m}^2$), stable DNI (fluctuations within a minute lower than $5 \text{ W}/\text{m}^2$).

3. Test campaign

3.1. Experimental setup

The vertically moving bar from the PETALES flux measurement system, with top speed over 2 m/s and position accuracy better than 0.1 mm with experimental load up to 100 kg, has been used to move all the sensors sequentially in the focal plane. Sensors were mounted on the water cooled protective shield “SNCF” that has been designed to protect the sides of the sensors. As the Big Solar Furnace in Odeillo has a large spot size (0.8 m diameter with mean 2000 kW/m²) when the full heliostat field is used (see Appendix A), extra care must be taken to protect the sensors, their wiring and tubing. The SNCF shield is a hollow aluminum plate (20 mm thick). Water as cooling liquid is passed through channels of variable depth. The layout of the individual channels has been designed based on CFD simulations in order to avoid low velocities areas hence hotspots due to localized poor cooling. The shield allows low and stable temperature around the sensors thanks to good cooling performance without hot spots. The front face that is exposed to concentrated solar radiation is made from an thin, polished copper plate electrolytically plated with nickel to maximize the reflectivity for solar radiation. With this the required cooling power can be kept acceptable. The SNCF provides holes to install 2 sensors of 25.4 mm in diameter, 1 sensor of 16 mm diameter, 1 50x50 mm separate water cooled target, and 2 calorimeters: the DLR SunCatch II [7] and the CNRS Idefix, see Fig. 2 b and c. The 50x50 mm opening houses an easily replaceable magnesium oxide smoked target to test the camera from the PETALES system and visually check the homogeneity of the solar flux on the surface of the sensors.

In front of the SNCF and the PETALES moving bar, a water cooled aluminum shield (2x2.5 m²) with a 500x150 mm² aperture was installed to protect the personnel and the data acquisition systems (see Fig. 2a), as the moving SNCF is too small to cover the complete focal area and, therefore, does not cover all the required surface.

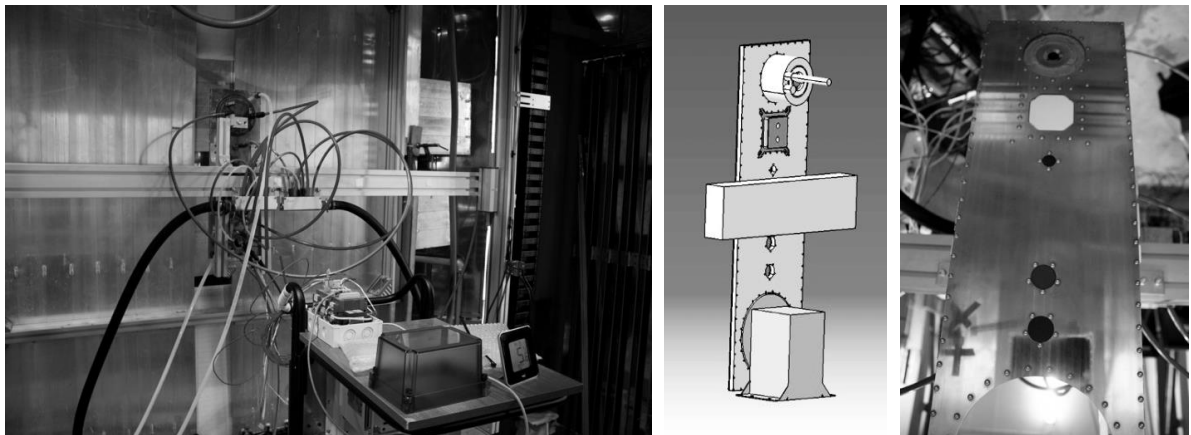


Fig. 2. (a) Part of the experimental setup as seen from the back: SNCF water-cooled shield with sensors installed on the moving bar behind the 2x2.5 m² water cooled aluminum shield with the failed central part exchanged with alumina insulation material that is visible at the bottom; (b) back of the water cooled protective shield SNCF with both planned calorimeters (including DLR SunCatch II not present in the results here); (c) close up from front of the SNCF with the 4 sensors actually compared, top to bottom: CNRS Idefix calorimeter, water cooled magnesium oxide smoke Lambertian white target, the 3 Gardon sensors (16 mm DLR, 25.4 mm PSI and 25.4 mm CIEMAT).

3.2. Experimental campaign

Three weeks had been reserved at the Big Solar Furnace in Odeillo in November and December 2012 for the campaign. Due to bad weather conditions, measurements could be performed during three days only. Tests at high power could be conducted only during the first two days, due to a catastrophic failure of the central part of the 2x2.5 m² water cooled shield. The damaged shield was replaced by high temperature alumina based insulation materials but further tests were limited to power levels of below 500 kW/m². These comparably low flux densities lead to low signals and noisy data most noticeable for the calorimeter. Hence rather high uncertainties result that could not be improved due to the limited availability of the facility.

For all the experiments, room temperature ranged from +5 to +9°C. No strong wind was observed, both in the heliostats field and at focus. Electronics were allowed at least 30 minutes warm-up before use. Inlet cooling tap water temperature for the sensors was stable, from +6 to +8°C.

The measurements have been done as fast as possible to reduce atmospheric and tracking error between the sensors but still having enough points (between 120 and 2500). Several configurations could be repeated twice.

4. Results and discussion

4.1. Uncertainties of the sensors and data evaluation

Calibration constants of the Gardon gages are given by the manufacturer Vatell as $\pm 3\% 1\sigma$. Accuracy of the data acquisition (voltage measurement) is stated by the manufacturer Gantner as $\pm 30 \mu\text{V } 6\sigma$ for our settings, with a repeatability $\pm 1 \mu\text{V } 2\sigma$ within 24 h. This excellent performance results in a very small influence of the accuracy of the voltmeter on the measured value for our campaign. Moreover the same device is used for all the sensors and its internal multiplexer is used to address the different sensors.

For the CNRS Idefix calorimeter, the determination of the total uncertainty is not as straightforward as for Gardon sensors. The uncertainty of the thermal power measured can be determined from the uncertainties of the temperature and the flow measurements. The error due to the apparent optical absorptivity of the cavity cannot be quantified. We have to assume that all the radiation passing through the aperture is transferred to the water based on the calculated absorptivity (>99%) and that reradiation losses are negligible.

The measured solar flux has been normalized for 1000 W/m^2 DNI based on the pyrheliometer measurements. Total absolute DNI uncertainty based on the manufacturers specification of the sensor and the voltmeter is $\pm 1.7\% 2\sigma$. Based on the characteristics of the DNI acquisition chain, short-term drifts have been neglected.

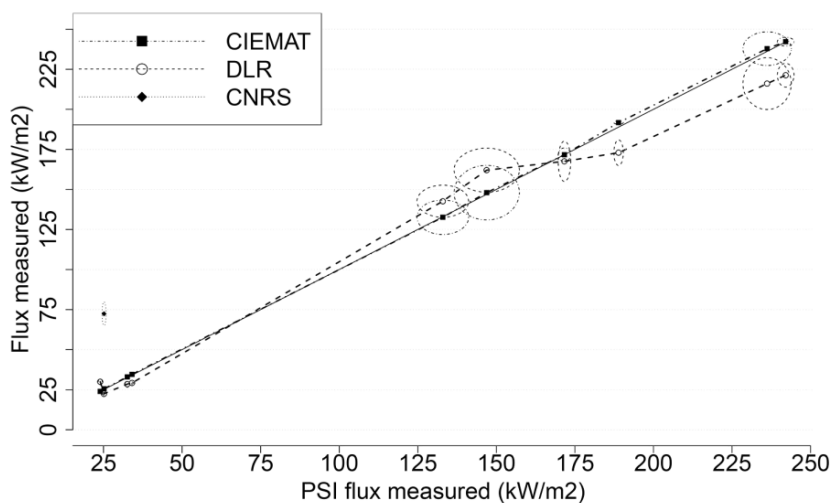


Fig. 3. Sensor response for different power levels relative to PSI sensor (solid black line).

Taking into account the points mentioned above we expect to benefit from an excellent short-term stability for all 4 sensor chains which allows well founded relative comparisons among them. In the data presented here we include 2σ error bars on both axis as ellipses from the statistic evaluation as presented in [12]. This should thus correspond to atmospheric or optical changes of the system rather than to inherent characteristics of the sensors, except for the low flux values where electrical and quantification noise is present ($< 50 \text{ kW/m}^2$ for our Gardon as here and $< 1000 \text{ kW/m}^2$ for the CNRS Idefix calorimeter). As none of the sensors to be compared is an official reference sensor we arbitrarily chose PSI's Gardon sensor as reference and report all data relative to this sensor.

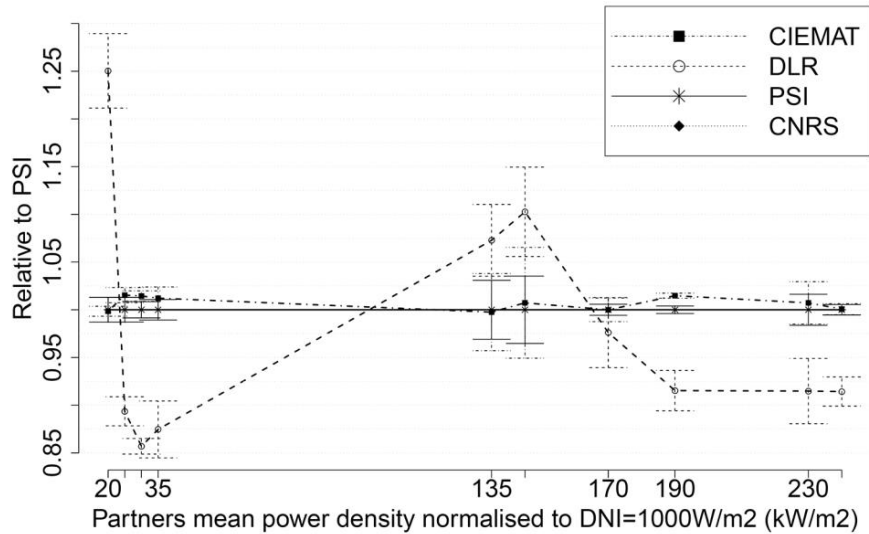


Fig. 4. Sensor response for different incoming beam angles relative to PSI sensor vs. angle.

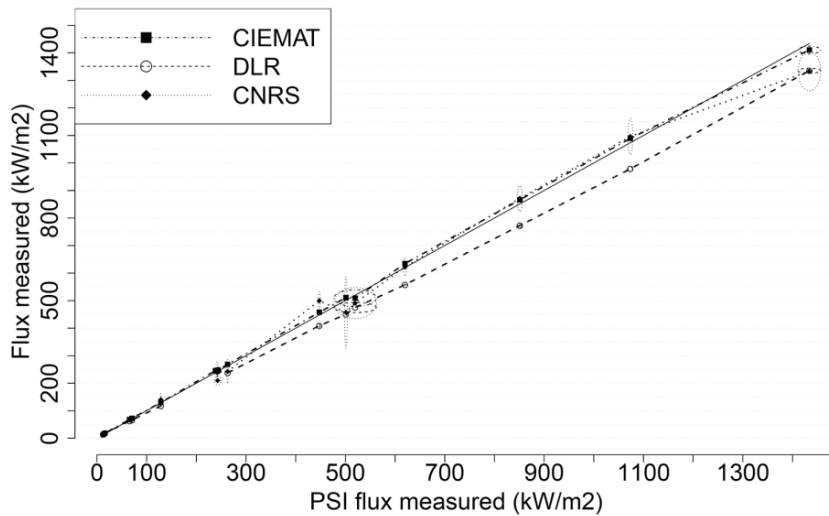


Fig. 5. Sensor response for different incoming beam angles relative to PSI sensor vs. power.

4.2. Observations

Summary of the results has been plotted in Fig. 3 to 5 with PSI's sensor as arbitrary reference. One observes:

- Data from CIEMAT's Gardon sensor with solar corrected calibration coefficient is typically 1% higher than PSI's Gardon sensor. The response of both sensors coincides within the statistical error even though PSI's calibration does include a systematic error in its calibration (see section 1.1.1).
- Data for DLR's Gardon sensor is typically 5-10% lower than PSI's Gardon for flux higher than 150 kW/m². This difference is statistically significant.
- Data for CNRS's Idefix calorimeter is very noisy but still is within 10% of PSI's sensor.

- PSI’s sensor reports a low value (-10%) relative to DLR’s or CIEMAT’s sensors for incoming radiation around an angle of 70°.

Based on our data, we report a maximum difference of 10% for flux densities up to 1500 kW/m² between the different sensors. With the limited amount of data available we can, at present, not assign these errors to either acquisition noise, the thermal stabilization of the sensors, or due to the solar furnace (tracking error, misalignment of heliostats due to wind load) or even small changes in atmospheric conditions.

The influence of the direction of the incoming radiation seems to be negligible (with the exception of the comparatively low value measured by PSI’s sensor around 70°). Also, cavity and flat sensors seems to exhibit a very similar angular response.

5. Conclusion and perspectives

This comparison of sensors based on different technologies and different calibration procedures shows an agreement within 10% of each other. The response of all sensors exhibits a negligible angular dependence.

Further work is required to pinpoint the origin of the 10% difference observed. The proposed simultaneous method might help for this. Furthermore, the data acquisition system might be optimized for low signals to improve the statistics of the experimental data. A low power calorimeter should also be included in future. Ideally, more data of more sensors should be acquired in a future campaign. This further work may help to separately quantify the errors associated with the solar furnace, the atmospheric changes or from sensor biases.

Acknowledgements

Financial support by the SFERA project (Grant Agreement no. 228296, work package 12 Flux & Temperature measurements) from the Research Infrastructures Activity in the 7th Framework Programme of the European Union is gratefully acknowledged. <http://sfera.sollab.eu>

The experimental campaign could not have existed without the work from Nicolas Boulet and Régis Rodriguez.

Appendix A. Geometry of the heliostats field of the Big Solar Furnace in Odeillo

The CNRS Big Solar Furnace in Odeillo (France), commissioned in 1972, has 63 flat heliostats with a total of 11340 flat mirrors to collect the solar energy, see Fig. 6. The complete heliostats field has a reflected beam surface over 2000 m² with a total mirror surface of 2835 m². The solar energy is then concentrated by a 54x40 m paraboloid with focus f=18 m and apparent surface of 1830 m². The paraboloid surface is made by 9500 silver mirrors individually bent to achieve high concentration ratio. Peak concentration ratio for the complete installation is 12000 kW/m², average concentration available on the complete 0.8 m diameter disk is 2000 kW/m². The total thermal power is 1 MW. All values are normalised for 1000 W/m² DNI. Exact day to day performance depends on the cleanliness and the canting of the mirrors of the heliostats which slightly evolve along the year: performance is estimated to be currently typically 10 to 20 % lower for both concentration and power characteristics.

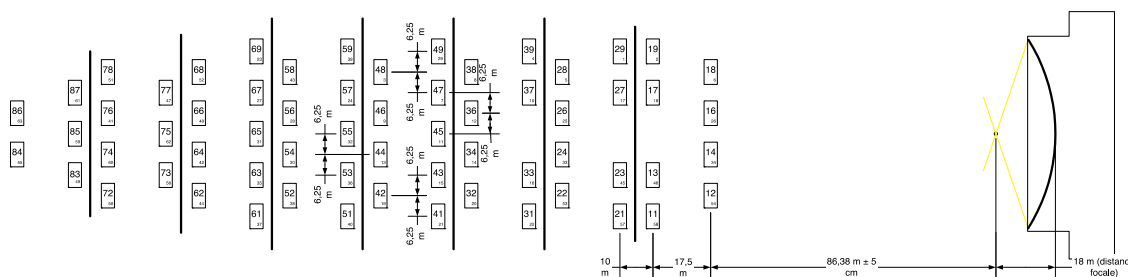


Fig. 6. Identification and relative position of the 63 heliostats and the parabola of the Big Solar Furnace.

Each heliostat is individually controlled by computer and can be used or not. As each heliostat is at a different distance to the parabola and impacts a different section of the parabola more or less tilted depending on the distance to the parabola focal axis (Fig. 6), each heliostat has a different contribution in density power and incoming angle at the focal plane. Power depends on the shadow between heliostats, which depends on their orientation: all the experiments were done with heliostats in solar tracking to minimize the shadow variation, either toward the paraboloid (in use) or below (not in use). The incoming angles at focus for each heliostat are presented in Fig. 7.

Vertical doors in high temperature steel in front of the focus protect the experimental area and allow another degree of power control by opening them more or less during solar operation of the heliostats, intercepting a varying part of the incoming beam energy.

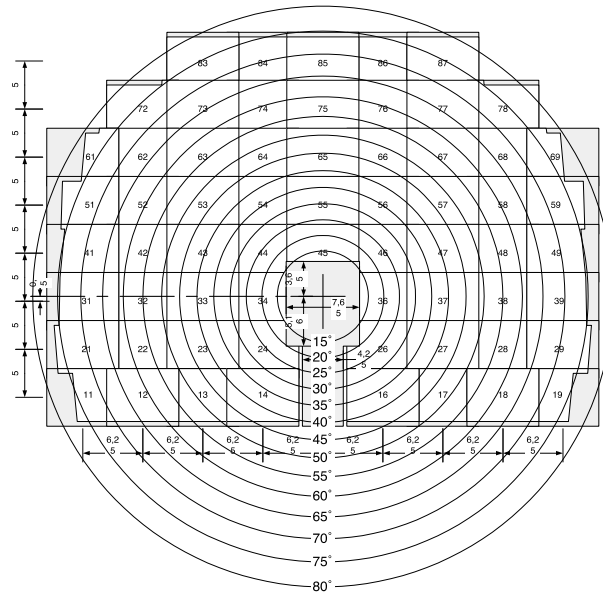


Fig. 7. Incoming beam angles at focus for each heliostat drawn on the parabola.

References

- [1] Kaluza J. and Neumann A., "Comparative measurements of different Solar flux gauge types", *Journal of Solar Engineering*, 2001, vol. 123, no3, pp. 251-255.
- [2] Andreas Neumann and Christian Willsch, "SolLab Radiometer Intercomparison Campaign 2006 Cologne", DLR Report.
- [3] J Ballestrín, S Ulmer, A Morales, A Barnes, L.W Langley, M Rodríguez, "Systematic error in the measurement of very high solar irradiance, *Solar Energy Materials and Solar Cells*", Volume 80, Issue 3, November 2003, Pages 375-381, ISSN 0927-0248, 10.1016/j.solmat.2003.08.014.
- [4] J. Ballestrín, M.Rodríguez-Alonso, J. Rodríguez, I. Cañadas, F. J. Barbero, L. W. Langley, A. Barnes "Calibration of high-heat-flux sensors in a solar furnace". *Metrologia* (Institute of Physics), Vol. 43, pp. 495 – 500, 2006. ISSN: 0026-1394
- [5] Gardon R., "An instrument for the direct measurement of intense thermal radiation", *Review of Scientific Instruments*, Vol. 24, No. 5, pp. 366-370, 1953.
- [6] Kendall, James M., "PRIMARY ABSOLUTE RADIOMETER", U.S. Patent No. 3,601,611, 24 Aug. 1971.
- [7] Willsch C., Dibowski G., « SFERA VTS - Verification Test SunCatch II », 2011
- [8] Ferriere, A., and B. Rivoire. "Measurement of concentrated solar radiation: the camorimeter ASTERIX." 10th International Symposium on Concentrated Solar Power and Chemical Energy Technologies, Australia. 2000.
- [9] Wilbert, S., Reinhardt, B., DeVore, J., Röger, M., Pitz-Paal, R., Gueymard, C., Buras, R. (2013). "Measurement of solar radiance profiles with the sun and aureole measurement system (SAM)." *Journal of Solar Energy Engineering* (in print).
- [10] Wilbert, S., Pitz-Paal, R., Jaus, J., (2012). Circumsolar Radiation and Beam Irradiance Measurements for Focusing Collectors. ES1002: COST WIRE Workshop May 22nd-23rd 2012, Risö.
- [11] Ulmer, Steffen, et al. "Calibration corrections of solar tower flux density measurements." *Energy* 29.5 (2004): 925-933.
- [12] NIST/SEMATECH e-Handbook of Statistical Methods, <http://www.itl.nist.gov/div898/handbook/>, last access in June 2013.